MOLECULAR AND CELLULAR BIOLOGY, July 2003, p. 4428–4438 Vol. 23, No. 13
0270-7306/03/$08.00+0 DOI: 10.1128/MCB.23.13.4428–4438.2003

Use of *Bmp1*/*Tll1* Doubly Homozygous Null Mice and Proteomics To Identify and Validate In Vivo Substrates of Bone Morphogenetic Protein 1/Tolloid-Like Metalloproteinases

William N. Pappano,[1] Barry M. Steiglitz,[1] Ian C. Scott,[2]† Douglas R. Keene,[3] and Daniel S. Greenspan[1,2]*

Departments of Biomolecular Chemistry[1] and Pathology and Laboratory Medicine,[2] University of Wisconsin, Madison, Wisconsin 53706, and Shriners Hospital for Children, Portland, Oregon 97201[3]

Received 29 January 2003/Returned for modification 17 March 2003/Accepted 26 March 2003

Bone morphogenetic protein 1 (BMP-1) and mammalian Tolloid (mTLD), two proteinases encoded by *Bmp1*, provide procollagen C-proteinase (pCP) activity that converts procollagens I to III into the major fibrous components of mammalian extracellular matrix (ECM). Yet, although *Bmp1*$^{-/-}$ mice have aberrant collagen fibrils, they have residual pCP activity, indicative of genetic redundancy. Mammals possess two additional proteinases structurally similar to BMP-1 and mTLD: the genetically distinct mammalian Tolloid-like 1 (mTLL-1) and mTLL-2. Mice lacking the mTLL-1 gene *Tll1* are embryonic lethal but have pCP activity levels similar to those of the wild type, suggesting that mTLL-1 might not be an in vivo pCP. In vitro studies have shown BMP-1 and mTLL-1 capable of cleaving Chordin, an extracellular antagonist of BMP signaling, suggesting that these proteases might also serve to modulate BMP signaling and to coordinate the latter with ECM formation. However, in vivo evidence of roles for BMP-1 and mTLL-1 in BMP signaling in mammals is lacking. To remove functional redundancy obscuring the in vivo functions of BMP-1-related proteases in mammals, we here characterize *Bmp1 Tll1* doubly null mouse embryos. Although these appear morphologically indistinguishable from *Tll1*$^{-/-}$ embryos, biochemical analysis of cells derived from doubly null embryos shows functional redundancy removed to an extent enabling us to demonstrate that (i) products of *Bmp1* and *Tll1* are responsible for in vivo cleavage of Chordin in mammals and (ii) mTLL-1 is an in vivo pCP that provides residual activity observed in *Bmp1*$^{-/-}$ embryos. Removal of functional redundancy also enabled use of *Bmp1*$^{-/-}$ *Tll1*$^{-/-}$ cells in a proteomics approach for identifying novel substrates of *Bmp1* and *Tll1* products.

Bone morphogenetic protein 1 (BMP-1), first identified as a protein of unknown function that copurifies with transforming growth factor beta (TGF-β)-like BMPs from osteogenic extracts of bone (38), is the prototype of a family of structurally similar metalloproteinases involved in morphogenesis in a broad range of species (4). Surprisingly, despite its association with TGF-β-like molecules, the first described role for BMP-1 was as a procollagen C-proteinase (pCP) (14, 17): the activity necessary for cleaving C-propeptides from type I to III procollagen precursors to produce mature monomers capable of forming the major collagen fibrils of vertebrate extracellular matrix (ECM) (25). A single gene encodes alternatively spliced RNAs for BMP-1 and for a second protease, mammalian Tolloid (mTLD) (35), that has been shown to have pCP activity in vitro (29, 17). Nevertheless, although embryos homozygous null for the *Bmp1* gene, which encodes both proteases, have abnormal collagen fibrils, mouse embryo fibroblasts (MEFs) derived from these embryos have residual pCP activity that is ~40% of that of the wild type (33), suggesting the existence of at least one additional mammalian pCP. Searches for additional mammalian BMP-1-related proteases identified two novel, genetically distinct proteases, mammalian Tolloid-like 1 and 2 (mTLL-1 and mTLL-2) (29, 34). Thus, mammals have a total of four BMP-1-related proteases, since additional mammalian BMP-1-related proteases are absent from the databases.

It has been demonstrated that mTLL-1 has pCP activity in vitro, while mTLL-2 reportedly lacks such activity (29). Nevertheless, mice homozygous null for the mTLL-1 gene (*Tll1*) have collagen fibrils of normal appearance, while *Tll1*$^{-/-}$ MEFs have pCP activity levels indistinguishable from wild-type levels (5). Such results have suggested that mTLL-1 might not operate as a pCP in vivo and have left open the question of which gene product(s) might provide residual pCP activity observed in *Bmp1*$^{-/-}$ MEF cultures.

Various proteins involved in ECM formation are synthesized as precursors, with propeptides that are proteolytically removed to yield mature functional forms. Some of these have cleavage sites with similarities to the cleavage sites of the procollagen I to III C-propeptides, and this has suggested them as possible candidate substrates of BMP-1-like proteases. Analyses of candidates identified in such an approach has now implicated the four mammalian BMP-1-related proteases in the biosynthetic processing of precursors to the mature forms of biglycan (31), laminin 5 (1), type VII collagen (26), and lysyl oxidase (37). Surprisingly, however, a site for cleavage of N-propeptides of type V procollagen by BMP-1 was found to be totally dissimilar to those of the procollagen I to III C-propeptides (13). Thus, comprehensive searches for novel substrates of BMP-1-like proteases must clearly be more unbiased in respect to the nature of cleavage sites.

* Corresponding author. Mailing address: Department of Pathology, University of Wisconsin, 1300 University Ave, Madison, WI 53706. Phone: (608) 262-4676. Fax: (608) 262-6691. E-mail: dsgreens@facstaff.wisc.edu.

† Present address: AstraZeneca R&D Charnwood, Loughborough, Leics LE11 5RH, United Kingdom.

The *Drosophila* BMP-1-related protease Tolloid, product of one of at least seven zygotically active genes involved in embryonic dorsal-ventral patterning (9), acts by cleaving the secreted protein Short gastrulation (SOG) (18) to release the TGF-β-like molecule Decapentaplegic (DPP) from a latent DPP-SOG complex. Similarly, the BMP-1-related nonmammalian vertebrate proteases *Xenopus* Xolloid (23) and zebrafish Tolloid (3) are capable of in vitro cleavage of the SOG orthologue *Xenopus* Chordin and of counteracting dorsalizing effects of Chordin upon co-overexpression of protease and Chordin in *Xenopus* (23) or zebrafish (3) embryos. Mammalian BMP-1 and mTLL-1 are capable of cleaving mammalian Chordin in vitro and of counteracting dorsalizing effects of mammalian Chordin upon co-overexpression in *Xenopus* embryos (29), while neither mTLD nor mTLL-2 cleaves or counteracts Chordin in similar assays (29). However, mTLD was recently shown to have some ability to process Chordin in vitro in the presence of the protein Twisted Gastrulation, which appears to affect both cleavage of Chordin by some BMP-1-related proteases and ability of Chordin to bind the vertebrate DPP orthologue BMP-4 (30). Importantly, despite insights provided by previous studies, no proofs exist as to which, if any, mammalian BMP-1-related proteases might actually act to modulate BMP signaling in vivo in the normal course of development and homeostasis.

In this report, embryos that are doubly homozygous null for both *Bmp1* and *Tll1* have been generated in an attempt to remove functional redundancy and, thereby, to resolve a number of outstanding questions regarding in vivo roles of mammalian BMP-1-related proteinases. Cells derived from these embryos are successfully used to demonstrate that products of *Bmp1* and *Tll1* are together responsible for in vivo processing of Chordin in mammals. *Bmp1*$^{-/-}$ *Tll1*$^{-/-}$ doubly null cells are also used to show mTLL-1 to be an in vivo pCP responsible for residual pCP activity in *Bmp1*$^{-/-}$ embryos, while separate biochemical analyses show for the first time that mTLL-2 has pCP activity in the presence of certain modifier proteins. Finally, proteomics-based analysis of *Bmp1*$^{-/-}$ *Tll1*$^{-/-}$ cells, rather than a candidate substrate approach, is used to identify a novel substrate for mammalian BMP-1-like proteases. Implications of the data are discussed.

MATERIALS AND METHODS

DNA analysis and genotyping. Tail biopsies or yolk sac fragments were lysed in a solution containing 100 mM Tris-HCl (pH 7.5), 50 mM EDTA, 0.5% sodium dodecyl sulfate (SDS), and 0.1 mg of proteinase K/ml and digested overnight at 59°C. DNA extracted with phenol-chloroform was precipitated with 75% ethanol and resuspended in water. Genotyping via PCR amplification used the following primers for *Bmp1* sequences: 5′-ACAGAACACCTTGTTCGACC-3′ (forward primer for both wild-type and mutant alleles), 5′-GCTGCCTGTGGAAGGAT AAGCTGG-3′ (reverse primer for wild-type allele only), and 5′-GCTATGAC CATGATTACGCC-3′ (reverse primer for null allele only). For *Tll1* sequences, primers were the following: 5′-GGTTACCCCTTCCTCTGCTTATGC-3′ (reverse primer for both wild-type and null alleles), 5′-GTCACCATCATTAGAG AGACCATCCAG-3′ (forward primer for wild-type allele only), and 5′-CGCT GCCTCGTCCTGCAGTTCATTCAG-3′ (forward primer for null allele only). Conditions for all PCR amplifications were 94°C for 5 min, followed by 32 cycles of 94°C for 30 s, 65°C for 30 s, and 72°C for 3 min, and a final extension at 72°C for 10 min. Products for *Bmp1* alleles were 600 bp (wild type) and 400 bp (null). Products for *Tll1* alleles were 900 bp (null) and 450 bp (wild type).

Preparation of MEFs. MEFs were prepared from mouse embryos at 13.5 days postcoitum (dpc), as previously described (12).

Electron microscopy. Embryo tail skin was prepared for electron microscopy by 60 min of fixation in 1.5% paraformaldehyde–1.5% glutaraldehyde in 0.1 M cacodylate buffer (pH 7.4) containing 0.05% tannic acid and 0.1% $CaCl_2$. Samples were rinsed in buffer, immersed for 60 min in 1.0% buffered OsO_4, rinsed again in buffer, dehydrated in a graded series of ethanol to 100%, infiltrated in propylene oxide, and embedded in Spurr's epoxy.

For immunoelectron microscopy, MEFs were grown on Thermanox coverslips (Nalge Nunc International), rinsed in serum-free Dulbecco's modified Eagle's medium (DMEM), and then incubated for 3 h at ambient temperature with rabbit polyclonal antibody LF-104 diluted 1:5 with serum-free DMEM. The antibody LF-104, directed against sequences in the probiglycan prodomain, has been described previously (11) and was the kind gift of Larry Fisher (National Institutes of Health, Bethesda, Md.). Cultures were rinsed for 30 min in serum-free DMEM and then incubated for 2 h in goat anti-rabbit 5-nm gold-conjugated secondary antibody (Amersham) diluted 1:10 in serum-free DMEM. Cells were then rinsed for 30 min in serum-free DMEM, fixed in 1.5% glutaraldehyde–1.5% paraformaldehyde, and further fixed, dehydrated, and embedded as described above for tissues.

Ultrathin sections were mounted on formvar-coated 1- by 2-mm slot grids, stained in saturated uranyl acetate dissolved in 50% ethanol, followed by Reynold's lead citrate, and then examined using a Philips EM410 transmission electron microscope operated at 80 kV. A full discussion of the outlined electron microscopy techniques may be found in reference 27.

Metabolic radiolabeling of MEFs. Confluent MEFs were metabolically radiolabeled essentially as in the work of Suzuki et al. (33). Briefly, MEFs were incubated for 24 h in a solution containing DMEM (pH 7.0), 10% fetal bovine serum (FBS), 25 μg of ascorbate/ml, and 100 μg of soybean trypsin inhibitor (SBTI) (Sigma)/ml, depleted in labeling medium (DMEM [pH 7.0], 5% dialyzed FBS, 25-μg/ml ascorbate; 100-μg/ml SBTI) for 2 h without isotope, and then radiolabeled 20 h with 20 μCi of L-(2,3-^{3}H)proline/ml. Protease inhibitors were added to harvested media to final concentrations of 25 mM EDTA, 1 mM *N*-ethylmaleimide (NEM), 1 mM *p*-aminobenzoic acid (PABA), 1 mM phenylmethylsulfonyl fluoride (PMSF), 10 μg of leupeptin/ml, and 5 μg of pepstatin/ml; and cell debris was removed by centrifugation. Collagenous forms were precipitated with 30% saturated ammonium sulfate on ice for 24 h, resuspended in 50 mM Tris-HCl (pH 7.5), 0.15 M NaCl, 25 mM EDTA, 1 mM NEM, 1 mM PABA, 1 mM PMSF, 10 μg of leupeptin/ml, and 5 μg of pepstatin/ml; reprecipitated with 3 volumes of ethanol; and analyzed by SDS-PAGE under reducing conditions on a 5% gel, and autofluorography as described by Lee et al. (16). Gel loadings were of samples derived from conditioned media of equal numbers of cells.

RT-PCR of MEF RNA. Total cell RNA was prepared from MEFs as described previously (31), using TRIzol reagent (Life Technologies, Inc.). Reverse transcription (RT) of 1 μg of RNA was performed using SuperScript II reverse transcriptase (Life Technologies, Inc.). Conditions for PCR were 94°C for 2 min, followed by 35 cycles of 94°C for 10 s, 65°C for 30 s, and 72°C for 2 min, and a final extension at 72°C for 10 min. Mouse Chordin-specific primers were 5′-GG ATTCTATGGCTCAGAGGCTCAGGG-3′ (forward) and 5′-TCTCCTGGCT CCAGATTTGGTAGGCTGG-3′ (reverse). Glyceraldehyde-3-phosphate dehydrogenase control primers were as previously described (31). Products were electrophoresed on a 1.5% agarose gel and visualized with ethidium bromide.

Isolation of MEF Chordin. MEFs, grown to confluence in DMEM–10% FBS, were washed three times with phosphate-buffered saline (PBS) and switched to serum-free DMEM containing 40 μg of SBTI/ml. After 16 h, heparin (Sigma) was added to media to a final concentration of 30 μg/ml, and 8 h after that, conditioned media were harvested and protease inhibitors were added to final concentrations of 1 mM PMSF, 1 mM NEM, 1 mM PABA, and 10 mM EDTA. Two hundred fifty microliters of a 50% heparin Sepharose slurry (CL-6B; Amersham Pharmacia Biotech) in PBS was added to 10 ml of conditioned medium from each genotype and rotated for 16 h at 4°C. Heparin Sepharose-containing media were centrifuged, supernatants were removed, and pellets were washed two times with 10 ml of PBS at 4°C. Two hundred microliters of 4× SDS-PAGE sample buffer–5% β-mercaptoethanol was added to each pellet, the resulting sample was mixed and boiled 5 min, and 20-μl aliquots were subjected to SDS-PAGE on 4 to 15% acrylamide gradient gels.

Immunodetection of MEF proα1(I)-derived collagen chains. MEFs were grown in DMEM–10% FBS to ~80% confluence and then switched to DMEM–10% FBS containing 50 μg of ascorbate/ml overnight. Cells were then washed three times with PBS and switched to serum-free media containing 50 μg of ascorbate/ml and 40 μg of SBTI/ml. Conditioned media were harvested, and proteinase inhibitors were added to final concentrations of 1 mM PMSF, 1 mM NEM, 1 mM PABA, and 10 mM EDTA. Media samples were prepared by addition of 4× SDS-PAGE sample buffer–5% β-mercaptoethanol and boiled for

5 min. Cell layers were washed three times with PBS and then collected immediately by scraping them into hot SDS-PAGE sample buffer–5% β-mercaptoethanol and boiling it for 5 min. Samples were subjected to SDS-PAGE on 5% acrylamide gels and to Western blot analysis, as described below.

Immunodetection of MEF proα1(XI)-derived collagen chains. Samples were prepared as described for isolation of type V collagen from MEF cultures (36). Cells were grown in DMEM–10% FBS to ~80% confluence and then switched to DMEM–10% FBS containing 50 μg of ascorbate/ml overnight. The next day, cells were switched to serum-free DMEM containing 1 ng of TGF-β1 (R&D)/ml, 40 μg of SBTI/ml, and 50 μg of ascorbate/ml with or without 20 μM decanoyl-RVKR-chloromethyl ketone (Bachem). Media were collected after 48 h, made 30% saturated with ammonium sulfate, and nutated overnight at 4°C. Samples were centrifuged at 38,581 × *g*, and pellets were washed three times in 12.5 mM Tris-HCl (pH 7.5)–75% ethanol at 4°C, resuspended in SDS-PAGE sample buffer–5% β-mercaptoethanol, and boiled for 5 min. Samples were subjected to SDS-PAGE on 4% acrylamide gels and Western blot analysis, as described below.

Immunoblot conditions. Transfer of samples to polyvinylidene difluoride membranes, incubations of blots with antibodies, and washes were as described previously (15). All antibodies used for blots were derived from polyclonal rabbit antisera. Antibodies against sequences in the human proα1(I) C-telopeptide (LF-67) and C-propeptide (LF-41) have been previously described (11) and were the kind gift of Larry Fisher (National Institutes of Health, Bethesda, Md.). Antibodies against sequences in the rat proα1(XI) globular variable subdomain, encoded by the rat α1(XI) gene exon 7, have been previously described (19) and were the kind gift of Nick Morris (Shriners Hospital for Children, Portland, Ore.).

For the present study, antibodies to the N terminus of mature mouse Chordin were raised against the peptide EPPALPIRSEKEPLPVRGAC, which corresponds to amino acid residues 30 to 48 in the published mouse Chordin sequence (22), plus an additional cysteine for coupling to keyhole limpet hemocyanin. Anti-Chordin antibodies were affinity purified on a column of the peptide immunogen coupled to resin, using previously described methodologies (15). As a control, to show similar levels of proteins loaded per lane, samples from the Chordin study were subjected to an immunoblot using anti-connective tissue growth factor antibody (Fig. 5B), kindly provided by FibroGen (South San Francisco, Calif.).

In vitro procollagen cleavage assay. ^{3}H-radiolabeled type I procollagen was prepared as previously described (29, 13), and 400 ng was incubated for 30 min at 37°C alone or in the presence of an equimolar amount (~133 ng) of recombinant PCPE1, prepared as previously described (32), in 50 mM Tris-HCl (pH 7.5)–150 mM NaCl. Recombinant mTLL-1 and mTLL-2 with COOH-terminal FLAG epitopes were prepared and purified as previously described (29), and 30 ng of one or the other was added to reactions, along with 0.1 M $CaCl_2$, to bring the final concentration to 5 mM $CaCl_2$. Samples were returned to 37°C for 14 h, and reactions were quenched by adding 10× concentrated SDS-PAGE sample buffer containing β-mercaptoethanol and boiling it for 5 min. Samples were subjected to SDS-PAGE on a 5% acrylamide gel, which was then treated with EN^{3}HANCE (DuPont) and exposed to film.

Two-dimensional (2D) electrophoresis. MEFs were grown to confluence in DMEM–10% FBS, switched to DMEM–10% FBS containing 50 μg of ascorbate/ml overnight, and then switched to serum-free DMEM. After 48 h, conditioned media were collected and proteinase inhibitors were added to final concentrations of 1 mM PMSF, 1 mM NEM, 1 mM PABA, and 10 mM EDTA. Proteins from MEF conditioned media were precipitated by addition of 75% ethanol and rocking overnight at 4°C. Samples were centrifuged at 72,128 × *g*, and pellets were resuspended in SDS-PAGE sample buffer–5% β-mercaptoethanol and boiled for 5 min. One hundred micrograms of protein from each MEF sample was used for 2D electrophoresis, performed according to the method of O'Farrell (20) by Kendrick Labs, Inc. (Madison, Wis.) as follows: isoelectric focusing was carried out in glass tubes of inner diameter 2.0 mm using 2.0% pH 3.5 to 10 ampholines (Amersham Pharmacia Biotech) for 9,600 V · h. Fifty nanograms of isoelectric focusing internal standard tropomyosin was added to each sample. This protein migrates as a doublet with a lower polypeptide spot of molecular weight ~33,000 and pI 5.2, marked by an arrow on the stained gels. After 10 min of equilibration in a solution containing 10% glycerol, 50 mm dithiothreitol, 2.3% SDS, and 0.0625 M Tris-HCl (pH 6.8), each tube gel was sealed to a stacking gel atop a 10% acrylamide slab gel (1 mm thick) and subjected to SDS-PAGE for ~4 h at 12.5 mA/gel. Silver-stained gels were dried between sheets of cellophane.

Mass-spectrometry sequencing. Excised spots were rehydrated, washed twice with 0.05 M Tris (pH 8.5)–30% acetonitrile and then with 100% acetonitrile for 1 to 2 min, lyophilized, and digested with 0.06 μg of sequencing grade modified trypsin (Roche Molecular Biochemicals) in 13 to 15 μl of 0.025 M Tris (pH 8.5) overnight at 32°C. Peptides were extracted twice with 50-μl aliquots of 50% acetonitrile–2% trifluoroacetic acid, desalted with a C18 ZipTip (Millipore), and eluted with 10 μl of acetonitrile, and the volume was reduced to ~2 μl on a Speed Vac concentrator (Savant) prior to injection. Samples were subjected to MS/MS sequence analysis on a Micromass Q-Tof hybrid quadrupole–time-of-flight mass spectrometer with a nanoelectrospray source at the Columbia University Protein Chemistry Core Facility. Processed files were submitted to a MASCOT search (Matrix Science Ltd.) (22a).

RESULTS

Similar morphologies of *Bmp1*$^{-/-}$ *Tll1*$^{-/-}$ doubly homozygous null and *Tll1*$^{-/-}$ singly homozygous null mice. The *Bmp1*$^{-/-}$ genotype leads to perinatal lethality, with persistent herniation of the gut and abnormal collagen fibrils (33), while the *Tll1*$^{-/-}$ genotype is embryonic lethal, with primary defects apparently confined to ectopia of heart and aorta and various heart malformations, the most prominent being incomplete formation of the interventricular septum (5). However, heterozygotes of each knockout line (maintained on an outbred Black Swiss background) appear grossly normal, survive to adulthood, and are fertile (5, 33). To generate embryos doubly homozygous null for both genes, *Bmp1*$^{+/-}$ and *Tll1*$^{+/-}$ heterozygotes were intercrossed, followed by crossing of F_1 *Bmp1*$^{+/-}$ *Tll1*$^{+/-}$ double heterozygotes, none of which had obvious abnormalities, to each other. Genotyping of weanling pups showed that only *Bmp1*$^{+/-}$ heterozygotes, *Tll1*$^{+/-}$ heterozygotes, *Bmp1*$^{+/-}$ *Tll1*$^{+/-}$ double heterozygotes, and wild-type animals had survived to this stage. Examination of embryos at 10.5, 13.5, and 14.5 dpc, by gross morphological inspection and by histological analysis of hematoxylin and eosin-stained fixed sections, found no observable differences between the phenotype of *Bmp1*$^{-/-}$ *Tll1*$^{-/-}$ doubly null embryos and the previously reported phenotype (5) of *Tll1*$^{-/-}$ embryos. As previously reported for *Tll1*$^{-/-}$ embryos (5), *Bmp1*$^{-/-}$ *Tll1*$^{-/-}$ doubly null embryos begin to develop signs of cardiac failure at ~10.5 dpc and by 13.5 dpc display a distinctive phenotype with secondary symptoms (e.g., marked edema) indicative of cardiac failure and primary defects confined to the aorta and heart. As previously reported for *Tll1*$^{-/-}$ embryos (5), the most consistently observed primary defects in *Bmp1*$^{-/-}$ *Tll1*$^{-/-}$ embryos were large defects of the muscular interventricular septum and mispositioning of the descending aorta to the center and the entire heart towards the left side of the mutant embryo (data not shown). Interestingly, *Bmp1*$^{-/-}$ *Tll1*$^{-/-}$ embryos did not display defects of the outflow tract septum, despite previous evidence that this structure has high levels of both *Tll1* and *Bmp1* expression and our previous suggestion that absence of defects of this structure in *Tll1*$^{-/-}$ embryos might result from functional substitution by *Bmp1* (5). Similarly, abnormalities were not noted in developing skeletal elements or neural tissues in which high levels of expression of both *Bmp1* and *Tll1* have previously been observed (5, 33–35), nor in the endothelial linings of developing blood vessels, in which expression domains of *Bmp1* and *Tll1* are also thought to overlap (5).

Electron microscopy has previously shown *Bmp1*$^{-/-}$ embryos to have collagen fibrils with an abnormal "barbed wire" appearance due to the presence of bumps or projections on their surfaces (33), while collagen fibrils of *Tll1*$^{-/-}$ embryos

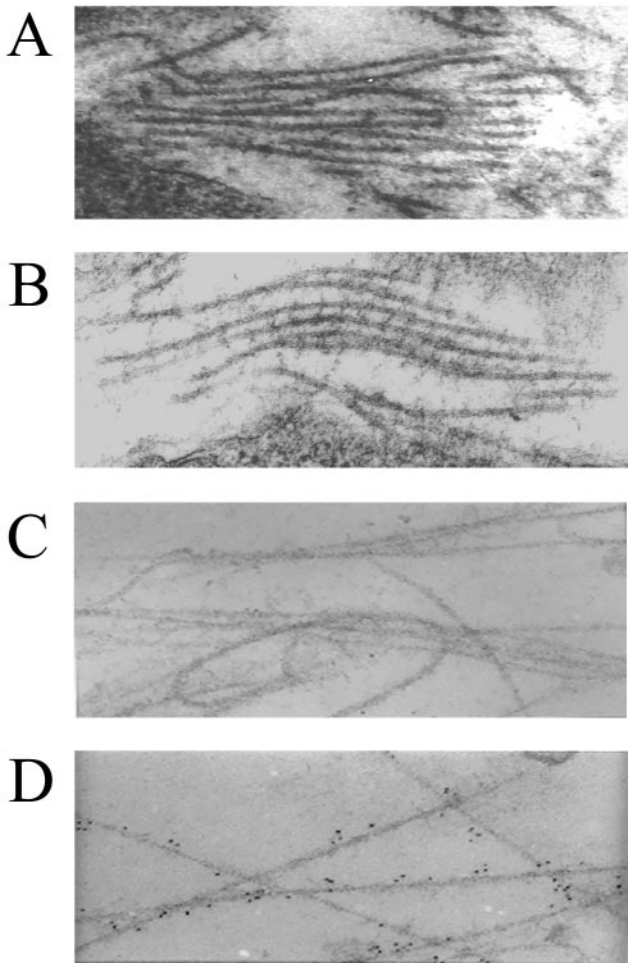

FIG. 1. *Bmp1*$^{-/-}$ *Tll1*$^{-/-}$ embryos form abnormal collagen fibrils with barbs that are associated with precursors of the proteoglycan biglycan. Electron micrographs show the ultrastructures of collagen fibrils near the dermal-epidermal junctions of 14.5-dpc wild-type (A) and *Bmp1*$^{-/-}$ *Tll1*$^{-/-}$ doubly null (B) embryo littermates and demonstrate immunolocalization of probiglycan to the barbs of abnormal collagen fibrils of the doubly null embryo (D) but not to fibrils of the wild-type littermate (C).

seemed normal in appearance (5). In the present study, transmission electron microscopy surprisingly found *Bmp1*$^{-/-}$ *Tll1*$^{-/-}$ embryos to have the same type of barbed wire collagen fibrils found in *Bmp1*$^{-/-}$ embryos (Fig. 1B). Thus, even in the absence of products of both *Bmp1* and *Tll1* genes, collagen fibrillogenesis is able to occur, albeit with the production of fibrils of abnormal morphology. These results suggested that either *Tll1* is not responsible for residual pCP activity noted in *Bmp1*$^{-/-}$ embryos (33) or that, in contradiction to accepted dogma, fibrillogenesis can occur in the total absence of cleavage of procollagen C-propeptides.

We have previously speculated that barbs on the abnormal collagen fibrils of *Bmp1*$^{-/-}$ embryos represent uncleaved C-propeptides of monomers incorporated into fibrils (33), and cell culture and biochemical studies in the present work are consistent with this possibility (see below). However, attempts in the present study to localize C-propeptides to barbs of collagen fibrils in *Bmp1*$^{-/-}$ *Tll1*$^{-/-}$ embryo tissues were unsuccessful, since available antibodies to a peptide corresponding to sequences in the C-propeptide of the proα1(I) chain of type I procollagen (11) proved unsuitable for immunohistochemistry and were unable to detect even the C-propeptides of intracellular procollagen molecules (data not shown). Surprisingly, however, in a survey with available antibodies directed against propeptides of other known substrates of BMP-1-like proteases, conducted to determine whether other uncleaved precursor molecules might accumulate and localize to structures in *Bmp1*$^{-/-}$ *Tll1*$^{-/-}$ embryo tissues, probiglycan, precursor of the small proteoglycan biglycan, was found by immunoelectron microscopy to be localized to the barbs of collagen fibrils in *Bmp1*$^{-/-}$ *Tll1*$^{-/-}$ embryo tissues (Fig. 1D). Thus, the barbs on abnormal *Bmp1*$^{-/-}$ *Tll1*$^{-/-}$ collagen fibrils appear to contain or be associated with at least one noncollagenous protein.

mTLL-1 is an in vivo pCP responsible for residual pCP activity in *Bmp1*$^{-/-}$ embryos. Sequences for mTLL-1 were originally isolated in a screen for proteases responsible for the residual pCP activity observed in *Bmp1*$^{-/-}$ MEF cultures (33, 34). However, although recombinant mTLL-1 has pCP activity in in vitro assays (29), *Tll1*$^{-/-}$ MEFs have levels of pCP activity indistinguishable from that of the wild type (5). To determine whether mTLL-1 is responsible for the residual pCP activity observed in *Bmp1*$^{-/-}$ MEFs, MEFs were derived from 13.5-dpc *Bmp1*$^{-/-}$ *Tll1*$^{-/-}$ doubly null embryos and assayed for processing of the C-propeptide of type I procollagen in culture media. In such assays, levels of pCP activity are evidenced by levels of mature type I collagen α1 and α2 chains, from which both N- and C-propeptides have been removed, and by levels of pNα1 and pNα2 processing intermediates, which retain N-propeptides but from which C-propeptides have been removed (Fig. 2A). Consistent with previous results (33), an autofluorogram of metabolically radiolabeled collagen forms from *Bmp1*$^{-/-}$ MEFs shows pCP activity to be reduced to ~40% of that of MEFs from a wild-type littermate. In contrast, however, mature α1(I) and α2(I) chains and pN forms, and thus pCP activity, are undetectable in media of *Bmp1*$^{-/-}$ *Tll1*$^{-/-}$ doubly null MEFs (Fig. 2B). Similarly, a Western blot (Fig. 2C) employing antibodies against sequences within the C-telopeptide region of the α1(I) chain found media of *Bmp1*$^{-/-}$ *Tll1*$^{-/-}$ doubly null MEFs to contain only intact proα1(I) chains and the processing intermediate pCα1(I), which retains the C-propeptide but from which the N-propeptide has been removed. In contrast, the same Western blot shows culture medium of MEFs from a wild-type littermate to contain predominantly fully processed mature α1(I) chains and a heavy band likely to represent a doublet containing both pCα1(I) forms and slightly smaller pNα1(I) forms, from which the C-propeptide has been removed but the N-propeptide retained. In the same blot, the size difference of pCα1(I) and pNα1(I) forms is displayed in a sample of partially processed human type I procollagen, run as a control (Fig. 2C). The markedly low levels of pCP activity in *Bmp1*$^{-/-}$ *Tll1*$^{-/-}$ doubly null MEF media, compared to levels found in *Bmp1*$^{-/-}$ MEF media (Fig. 2), shows mTLL-1 to be an in vivo pCP responsible for residual pCP activity found in *Bmp1*$^{-/-}$ MEFs.

Since cleavage of the C-propeptide is thought to be necessary for fibrillogenesis to occur (24), it seemed paradoxical that *Bmp1*$^{-/-}$ *Tll1*$^{-/-}$ doubly null embryos would form collagen

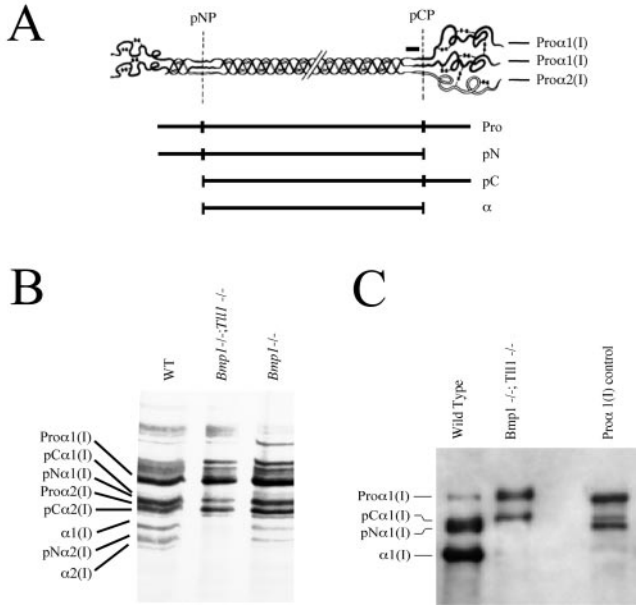

FIG. 2. *Bmp1*$^{-/-}$ *Tll1*$^{-/-}$ MEF culture medium lacks detectable pCP activity: mTLL-1 is an in vivo pCP. (A) A schematic of type I procollagen [a heterotrimer comprising two proα1(I) chains and one proα2(I) chain] illustrates positions of the pNP and pCP cleavage sites, for proteolytic removal of N- and C-propeptides, respectively. A horizontal black bar over the proα1(I) C-telopeptide domain (a small globular region, which is retained on mature α chains, between the triple-helical domain and the pCP cleavage site) marks the approximate position of amino acid residues corresponding to a peptide used as an immunogen to produce the antibodies (11) used in the Western blot of panel C. Represented diagrammatically below the procollagen schematic are the various procollagen biosynthetic cleavage products (Pro, procollagen; pN, form from which the C- but not N-propeptide has been removed; pC, form from which the N- but not C-propeptide has been removed; α, chains which constitute the mature triple-helical collagen monomer. (B) An autofluorogram is shown of metabolically radiolabeled procollagen and collagen processing intermediates in the conditioned media of wild-type (WT), *Bmp1*$^{-/-}$ *Tll1*$^{-/-}$, and *Bmp1*$^{-/-}$ MEF cultures. pNα1(I) forms many times comigrate with proα2(I) forms on gels. Thus, it is most probable that the seemingly single band labeled as both pNα1(I) and proα2(I) represents both pNα1(I) and proα2(I) forms in the WT and *Bmp1*$^{-/-}$ lanes, in which this band is dark, and only the proα2(I) form in the *Bmp1*$^{-/-}$ *Tll1*$^{-/-}$ lane, in which this band is light. (C) A Western blot shows proα1(I) chains and processing products detected in conditioned media of wild-type and *Bmp1*$^{-/-}$ *Tll1*$^{-/-}$ MEF cultures.

fibrils, albeit morphologically abnormal fibrils (Fig. 1), in the apparently total absence of pCP activity (Fig. 2). To further examine the nature of *Bmp1*$^{-/-}$ *Tll1*$^{-/-}$ type I collagen fibrils, we characterized collagen forms incorporated into the ECM associated with MEF cell layers. As can be seen on a Western blot using the α1(I) C-telopeptide antibodies (Fig. 3A), both wild-type and *Bmp1*$^{-/-}$ *Tll1*$^{-/-}$ MEF cell layers contain completely unprocessed proα1(I) chains, which are likely to be intracellular. Both wild-type and *Bmp1*$^{-/-}$ *Tll1*$^{-/-}$ MEF cell layers also contain processing intermediates. Those in wild-type MEF matrix are likely pNα1(I) chains, since their mobilities are similar to those of pNα1(I) chains in a control sample of partially processed type I procollagen (Fig. 3A) and because various experimental approaches have previously found pC forms to be absent from normal collagen fibrils (15, 24). In regard to the latter point, it was especially interesting that processing intermediates in *Bmp1*$^{-/-}$ *Tll1*$^{-/-}$ MEF ECM have mobilities slower than those of the pNα1(I) chains in both the wild-type sample and the partially processed procollagen control and similar to the mobility of pCα1(I) chains in the control sample (Fig. 3A). To ascertain whether processing intermediates in *Bmp1*$^{-/-}$ *Tll1*$^{-/-}$ MEF matrix did, in fact, correspond to pCα1(I) chains, Western blot analysis was performed using antibodies directed against proα1(I) C-propeptide sequences. As can be seen (Fig. 3B), pCα1(I) chains were detected in *Bmp1*$^{-/-}$ *Tll1*$^{-/-}$ MEF cell layer ECM but, as expected, were absent from wild-type MEF ECM. These findings are consistent with the probability that the barbed collagen fibrils in *Bmp1*$^{-/-}$ *Tll1*$^{-/-}$ embryos contain monomers with retained C-propeptides.

In addition to pCα1(I) forms, the Western blot of Fig. 3A also detected small amounts of forms the size of mature α1(I) chains in *Bmp1*$^{-/-}$ *Tll1*$^{-/-}$ ECM. Thus, low level C-propeptide processing appears to be occurring. This suggested either that doubly null MEFs have low levels of residual pCP activity or that C-propeptide removal had occurred via some alternative protease activity. Previous studies by members of this and another group (2, 16) have found that procollagen C-propeptides can be removed in cell cultures via a cell layer-associated activity that cleaves within the telopeptide at a site a few amino acid residues removed from the authentic pCP site used for in vivo removal of C-propeptides. However, such cleavage has been reported only in cell cultures to which neutral polymers have been added and results in α chains with slightly higher electrophoretic mobilities than those of α chains produced via cleavage by authentic pCP activity (2, 16). The α1(I) chains in *Bmp1*$^{-/-}$ *Tll1*$^{-/-}$ MEF ECM have a mobility similar to that of α1(I) chains in wild-type ECM (Fig. 3A). In addition, culturing *Bmp1*$^{-/-}$ *Tll1*$^{-/-}$ MEFs in pH 7.0 medium in the presence of soybean trypsin inhibitor, conditions which have been shown to inhibit the cell layer-associated telopeptidase activity (2, 16), had no apparent effect on collagen forms incorporated into cell layer-associated ECM (data not shown). These various results suggested that residual pCP activity, rather than an alternative cell layer-associated activity, was responsible for the low-level

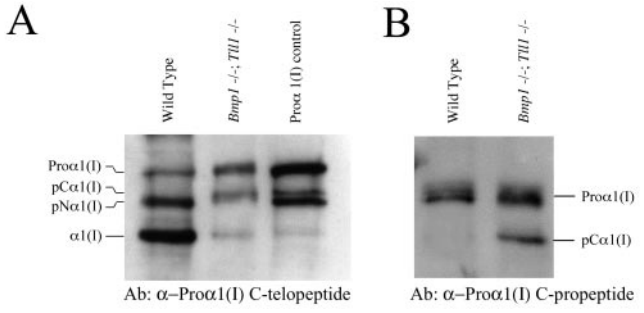

FIG. 3. *Bmp1*$^{-/-}$ *Tll1*$^{-/-}$ MEFs incorporate pC collagen forms, with uncleaved C-propeptides, and small amounts of apparently mature monomers into ECM. Western blots using antibodies directed against sequences in the proα1(I) C-telopeptide (A) or C-propeptide (B) demonstrate incorporation of pCα1(I) chains (A and B) and chains the size of mature, fully processed α1(I) chains into ECM associated with *Bmp1*$^{-/-}$ *Tll1*$^{-/-}$ MEF cell layers.

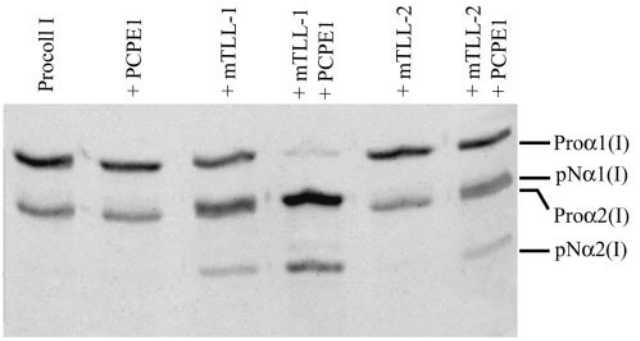

FIG. 4. Metalloproteinase mTLL-2 has detectable pCP activity in vitro in the presence of PCPE1. An autofluorogram of purified human type I procollagen incubated alone (Procoll I) or in the presence of PCPE1, mTLL-1, mTLL-2, or combinations of mTLL-1 plus PCPE1 or mTLL-2 plus PCPE1 is shown.

C-propeptide processing necessary to produce the α1(I) chains found in *Bmp1*$^{-/-}$ *Tll1*$^{-/-}$ MEF ECM.

mTLL-2 can function as a pCP. We were previously unable to detect mTLL-2 pCP activity in the types of in vitro assays used successfully to demonstrate pCP activity for BMP-1, mTLD, and mTLL-1 (29). However, since we have previously demonstrated expression of mTLL-2 RNA in MEFs (31), we sought other assay conditions which might reveal mTLL-2 pCP activity in order to determine whether mTLL-2 might be capable of providing low levels of residual pCP activity, thus accounting for the α1(I) chains in *Bmp1*$^{-/-}$ *Tll1*$^{-/-}$ MEF ECM. Procollagen C-proteinase enhancer 1 (PCPE1) is one of two secreted glycoproteins, each of which is capable of potentiating the activity of pCPs up to 1 order of magnitude under certain conditions (32). As can be seen (Fig. 4), in the presence of PCPE1, recombinant mTLL-2 has low but detectable levels of pCP activity in an in vitro assay. Thus, since MEFs secrete high levels of PCPE1 (data not shown), mTLL-2 may possibly furnish low levels of pCP activity responsible for the small amounts of α1(I) chains found in *Bmp1*$^{-/-}$ *Tll1*$^{-/-}$ MEF ECM.

Products of the *Bmp1* and *Tll1* genes are responsible for in vivo processing of Chordin. Availability of embryos with null *Bmp1* and *Tll1* alleles suggested the possibility of using tissues or cells from such embryos to resolve the question of whether products of the *Bmp1* and/or *Tll1* genes are actually responsible for in vivo processing of Chordin in mammals. RT-PCR demonstrated that wild-type, *Tll1*$^{-/-}$, *Bmp1*$^{-/-}$, and *Bmp1*$^{-/-}$ *Tll1*$^{-/-}$ doubly null MEFs all produce Chordin RNA (Fig. 5A). Thus, antibodies were raised against mouse Chordin sequences, and affinity-purified antibodies were employed for Western blots to compare levels of Chordin in the culture media of MEFs of the four different genotypes. Although Chordin was not detectable above background in Western blots of total proteins precipitated from MEF media with ethanol or trichloroacetic acid (data not shown), endogenous Chordin was detectable when removed from media using heparin Sepharose beads. As can be seen (Fig. 5B), full-length Chordin was not clearly detectable in medium of MEFs derived from wild-type or *Tll1*$^{-/-}$ littermate embryos. In contrast, however, full-length Chordin and a possible cleavage product are faintly visible in medium of MEFs derived from a *Bmp1*$^{-/-}$ littermate embryo, and full-length Chordin is clearly visible in medium from *Bmp1*$^{-/-}$ *Tll1*$^{-/-}$ doubly null MEFs. These results indicate products of both *Bmp1* and *Tll1* to be responsible for in vivo cleavage of Chordin in mammals.

A proteomics-based analysis of *Bmp1*$^{-/-}$ *Tll1*$^{-/-}$ doubly null MEFs identifies type XI collagen as a novel substrate for mammalian BMP-1-like proteases. The large differences in degrees of processing of procollagen I and Chordin in *Bmp1*$^{-/-}$ *Tll1*$^{-/-}$ doubly null MEF medium, compared to results with the wild type, suggested that cleavage products of various substrates represented as spots on 2D gels of wild-type MEF medium might be absent from 2D gels of *Bmp1*$^{-/-}$ *Tll1*$^{-/-}$ MEF medium. If so, such gels could be used in a

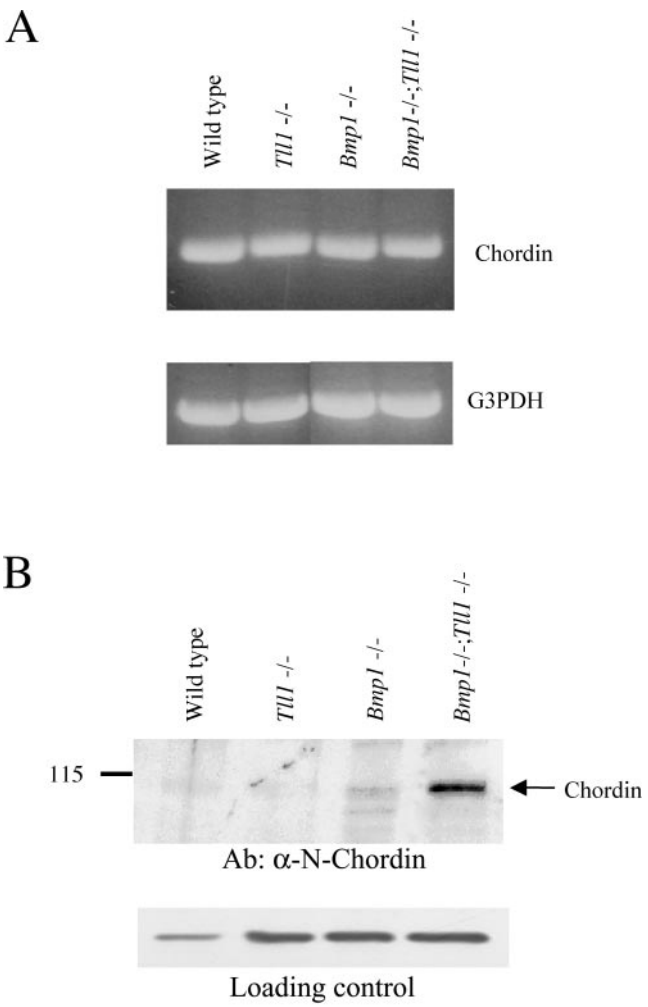

FIG. 5. Expression and processing of Chordin in cultures of MEFs with differing genotypes at the *Bmp1* and *Tll1* loci. (A) RT-PCR was employed to assay for possible MEF expression of Chordin RNA (upper panel) and for MEF expression of glyceraldehyde-3-phosphate dehydrogenase (G3PDH) RNA (lower panel) as a control for possible variations in RNA isolation, RT efficiency, and gel loading. (B) Western blot analysis was employed to assay for the presence of Chordin protein in MEF conditioned media, and the number 115 to the left of the blot marks the position of the molecular weight protein standard β-galactosidase (upper panel). As a control, to show that similar levels of protein were loaded per sample, the same samples were subjected to a Western blot employing antibodies to the unrelated protein connective tissue growth factor (lower panel).

proteomics approach towards identifying novel substrates of products of the *Bmp1* and *Tll1* genes. To ascertain the feasibility of such an approach, proteins from conditioned media of wild-type and *Bmp1*$^{-/-}$ *Tll1*$^{-/-}$ MEFs were separately subjected to 2D electrophoresis, and the patterns of spots were compared. Comparison identified a number of spots on the wild-type 2D gel (Fig. 6A) that were not detectable on the *Bmp1*$^{-/-}$ *Tll1*$^{-/-}$ gel (Fig. 6B), and a number of these were excised for analysis by mass spectrometry. Spots A, B, and C appeared to be part of separate series of spots of the same molecular weights, but different pIs, suggestive of differently charged versions of the same proteins. Mass spectrometry identified spot A as the C-propeptide of the proα1 chain of type I procollagen, spot B as the C-propeptide of the proα1 chain of type III procollagen, and spot C as the C-propeptide of the proα2 chain of type I procollagen. Thus, appearance of the C-propeptides of the major fibrillar collagens on the wild-type gel, but not the *Bmp1*$^{-/-}$ *Tll1*$^{-/-}$ gel, validates this approach as a means of identifying in vivo substrates of *Bmp1* and *Tll1* gene products. Mass spectrometry identified spot D as the proline- and arginine-rich protein (PARP) subdomain of the N-terminal globular sequences of the proα1 chain of type XI collagen, which has not previously been shown to be a substrate of BMP-1-like proteases.

N-propeptide of the proα1 chain of type XI collagen is an in vivo substrate for products of the *Bmp1* and *Tll1* genes. Type XI collagen is a low-abundance fibrillar collagen composed of heteromeric monomers containing α1(XI), α2(XI), and α3(XI) chains. The proα1 and proα2 chains of type XI procollagen differ from the proα chains of the major fibrillar collagens I to III in having larger and more complex N-terminal globular domains. The latter, as shown for the proα1(XI) chain (Fig. 7A), are composed of PARP and variable subdomains. We have previously demonstrated that the PARP domain of the proα1 chain of the low-abundance fibrillar collagen, type V, is cleaved by BMP-1-like proteases and that the C-propeptide is cleaved by furin-like proprotein convertase activity (13, 36). To further investigate the possibility of in vivo cleavage of the proα1(XI) PARP subdomain by *Bmp1* and *Tll1* gene products and to test whether the C-propeptide might be cleaved by furin-like activity, Western blot analysis was performed to compare processing of the proα1(XI) chain in wild-type and *Bmp1*$^{-/-}$ *Tll1*$^{-/-}$ MEF cultures in the presence and absence of furin inhibitor (Fig. 7B). In the absence of furin inhibitor, medium from wild-type MEFs contains five bands detectable by antibodies directed against sequences in the proα1(XI) variable subdomain. The two smallest bands correspond in size to mature α1(XI) chains, from which both PARP and C-propeptide domains have been cleaved (Fig. 7A). There are thought to be two size classes of α1(XI) chains due to alternative splicing which occurs within the variable subdomain (21, 40). Interestingly, in the absence of furin inhibitor, *Bmp1*$^{-/-}$ *Tll1*$^{-/-}$ MEF medium contained only two detectable bands, neither of which corresponded in size to mature α1(XI) chains. Thus, proteases produced by *Bmp1* and/or *Tll1* are responsible for processing proα1(XI) chains in MEF cultures.

By analogy to proteolytic processing of type V procollagen (36), it seemed likely that the two bands in *Bmp1*$^{-/-}$ *Tll1*$^{-/-}$ MEF medium represented pNα1(XI) forms which, in the absence of *Bmp1* and *Tll1* gene products, retained PARP domains but from which C-propeptides had been removed by furin-like convertase activity. Indeed, when the highly specific furin inhibitor decanoyl-RVKR-chloromethyl ketone is added to *Bmp1*$^{-/-}$ *Tll1*$^{-/-}$ MEF cultures, the two bands present in untreated *Bmp1*$^{-/-}$ *Tll1*$^{-/-}$ MEF medium disappear, to be replaced by two larger bands consistent in size with alternatively spliced forms of full-length proα1(XI) chains. Taken together, results of the Western blot thus indicate proα1(XI) chains to be cleaved at one end by product(s) of *Bmp1* and/or *Tll1* and at the other end by furin-like activity. Absence of the proα1(XI) PARP domain from the *Bmp1*$^{-/-}$ *Tll1*$^{-/-}$ 2D gel of Fig. 6 is consistent with the interpretation that this is the domain cleaved by BMP-1-like proteases and that the C-propeptide is cleaved by the furin-like activity.

DISCUSSION

Surprisingly, we show the morphology of *Bmp1*$^{-/-}$ *Tll1*$^{-/-}$ doubly null embryos to not differ in an obvious way from the previously described morphology of *Tll1*$^{-/-}$ embryos. This disproves previous predictions (5) that absence in *Tll1*$^{-/-}$ embryos of defects in outflow tract septum, major blood vessels, neural tissue, and cartilage, which normally show high levels of *Tll1* expression, might be due to functional compensation by *Bmp1*. Yet despite morphological similarities between *Tll1*$^{-/-}$ and *Bmp1*$^{-/-}$ *Tll1*$^{-/-}$ embryos, a series of analyses presented here show functional redundancy to have been sufficiently removed as to enable use of *Bmp1*$^{-/-}$ *Tll1*$^{-/-}$ doubly null embryo cells in addressing unanswered questions regarding in vivo functions of the mammalian BMP-1/Tolloid-related proteinases. Moreover, removal of functional redundancy has allowed use of *Bmp1*$^{-/-}$ *Tll1*$^{-/-}$ doubly null cells as tools in a proteomics approach towards identifying novel substrates of *Bmp1* and *Tll1* gene products.

The presence of residual pCP activity in *Bmp1* null embryos originally led to the search for additional mammalian BMP-1/Tolloid-related metalloproteases and to the isolation of mTLL-1 sequences (33, 34). Nevertheless, despite the finding

FIG. 6. Two-dimensional electrophoretic comparison of proteins in conditioned media of wild-type (A) and *Bmp1*$^{-/-}$ *Tll1*$^{-/-}$ doubly null (B) MEF cultures. Silver-stained, second-dimension SDS-PAGE slab gels are shown, with edges corresponding to the acidic ends of first-dimension isoelectric focusing gels to the left. Arrows mark the position on each gel of the ~33,000, pI-5.2 isoelectric focusing internal standard tropomyosin, added to each sample. Circles denote spots in the gel of wild-type conditioned medium (A) excised for mass-spectrometric analysis and corresponding positions in the gel of *Bmp1*$^{-/-}$ *Tll1*$^{-/-}$ doubly null conditioned medium (B). Mass-spectrometric analysis showed spots A, B, and C from the wild-type medium gel to correspond to C-propeptides of the proα1(I), proα1(III), and proα2(I) procollagen chains and showed spot D to correspond to the N-terminal globular PARP subdomain of the proα1(XI) procollagen chain, a novel substrate. Numbers to the right of the gels mark positions of molecular weight protein standards added to the agarose used to seal the tube gel to the slab gel: catalase (60,000), actin (43,000), carbonic anhydrase (29,000), and lysozyme (14,000).

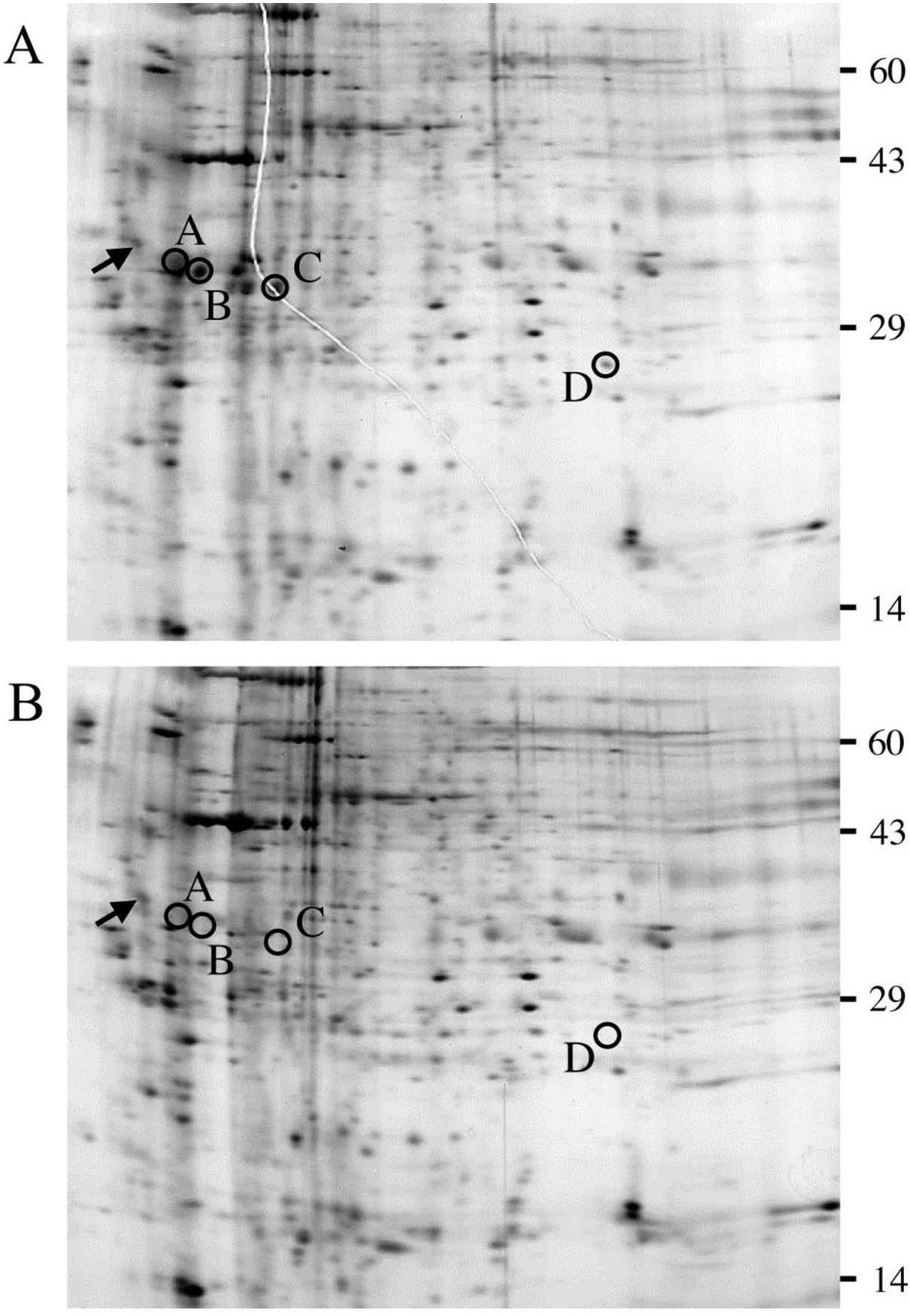
A
60
43
29
14
A
B
C
D
B
60
43
29
14
A
B
C
D

that recombinant mTLL-1 has detectable pCP activity in vitro (29), *Tll1*$^{-/-}$ embryos had collagen fibrils of normal appearance, while MEFs derived from these embryos had levels of pCP activity indistinguishable from those of wild-type littermates (5). Here we have employed characterization of *Bmp1*$^{-/-}$ *Tll1*$^{-/-}$ MEFs to demonstrate that the residual pCP activity observed in *Bmp1*$^{-/-}$ MEF culture media is provided by mTLL-1. Thus, mTLL-1 is an in vivo pCP, and products of the *Bmp1* and *Tll1* genes together appear responsible for all observable pCP activity in MEF culture media. The previous finding that recombinant BMP-1 has more robust pCP activity in vitro than does recombinant mTLL-1 (29) suggests that pCP levels in *Tll1*$^{-/-}$ MEF media may have appeared indistinguishable from the wild type (5; also data not shown), since the more robust pCP activity of BMP-1, combined with that of mTLD, is sufficient to fully compensate for loss of mTLL-1 pCP activity in *Tll1*$^{-/-}$ MEFs within the detection limits of our assays.

Although pCP activity is undetectable in *Bmp1*$^{-/-}$ *Tll1*$^{-/-}$ MEF culture medium, *Bmp1*$^{-/-}$ *Tll1*$^{-/-}$ embryos, nevertheless, form collagen fibrils. This suggested either that, in contradiction to accepted dogma, fibrillogenesis can occur in the total absence of procollagen C-propeptide cleavage or that some residual cleavage of C-propeptides occurs in these embryos. Examination of ECM associated with *Bmp1*$^{-/-}$ *Tll1*$^{-/-}$ MEF cell layers showed it to contain pCα forms, consistent with the probability that collagen monomers with uncleaved C-propeptides can, at least under certain circumstances, be incorporated into fibrils and that the barbed fibrils of *Bmp1*$^{-/-}$ *Tll1*$^{-/-}$ embryos contain collagen monomers with uncleaved C-propeptides. However, *Bmp1*$^{-/-}$ *Tll1*$^{-/-}$ MEF ECM also appeared to contain small amounts of collagen monomers of the same apparent size as monomers cleaved by authentic pCP activity at the physiologically relevant site, suggesting low levels of residual pCP activity. In contrast to previous results (29), mTLL-2 is demonstrated here to be capable of pCP activity, albeit at relatively low levels detectable in vitro only in the presence of the pCP potentiator PCPE1. Thus, since mTLL-2 RNA and PCPE1 have both been found to be expressed by MEFs, this combination of proteins may provide the low levels of apparent residual pCP activity. It is not entirely clear why mature collagen monomers are detectable in ECM, but not media, of *Bmp1*$^{-/-}$ *Tll1*$^{-/-}$ MEFs, although such enrichment in the ECM may reflect preferential incorporation of the small numbers of mature monomers, compared to incorporation of processing intermediates, into growing fibrils.

Although antibodies raised against a peptide corresponding to sequences within the type I procollagen C-propeptide did not prove suitable for immunohistochemistry, a survey with antibodies directed against the propeptides of other known substrates of BMP-1-like proteins, designed to localize uncleaved precursors in *Bmp1*$^{-/-}$ *Tll1*$^{-/-}$ tissues, did localize probiglycan, precursor of the small proteoglycan biglycan, to *Bmp1*$^{-/-}$ *Tll1*$^{-/-}$ collagen fibril barbs, which are thought to represent uncleaved procollagen C-propeptides. Biglycan has been reported to be capable of binding normal collagen fibrils (28). However, the suggestion from data presented here of an interaction between probiglycan and the type I procollagen C-propeptide was unexpected and of unknown significance. Since biglycan has been shown to be a positive regulator of bone growth (39), further studies into the nature of probiglycan-biglycan interactions with procollagen C-propeptides and possible effects on collagen biosynthesis are warranted.

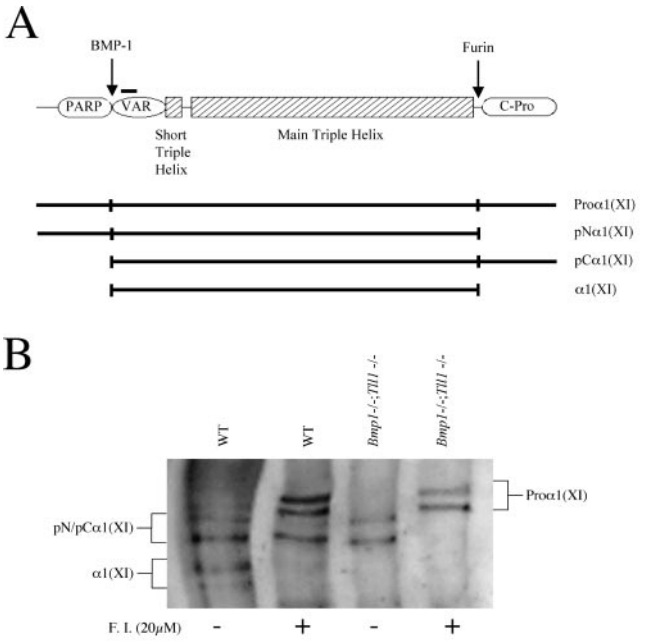

FIG. 7. Proα1(XI) chains are biosynthetically processed by BMP-1-like and furin-like proteases. (A) A schematic of the proα1(XI) chain illustrates sites for in vivo processing by BMP-1- and furin-like proteases, predicted on the basis of data presented in panel B and in Fig. 6. PARP and variable (VAR) subdomains and the C-propeptide (C-Pro) of the proα1(XI) chain are labeled. A horizontal black bar over the proα1(XI) variable domain marks the approximate position of amino acid residues corresponding to a peptide immunogen used to produce the antibodies (19) used in the Western blot of panel B. (B) Western blot analysis of processing of endogenous proα1(XI) chains in cultures of wild type (WT) or *Bmp1*$^{-/-}$ *Tll1*$^{-/-}$ doubly homozygous null MEFs in either the presence (+) or absence (−) of the furin inhibitor (F.I.) decanoyl-RVKR-chloromethyl ketone. The various proα1(XI) biosynthetic cleavage products labeled in panel B are represented diagrammatically beneath the schematic in panel A. pN/pCα1(XI), similarity in electrophoretic mobilities of pNα1(XI) and pCα1(XI) processing intermediates prevented distinguishing between them on the blot in panel B.

Both biochemical and genetic evidence supports an in vivo role for *Drosophila* Tolloid in regulating DPP signaling via cleavage of the DPP antagonist, and Chordin orthologue, SOG (18). Biochemically, *Xenopus* Xolloid, zebrafish Tolloid, mammalian BMP-1, and mTLL-1 have been shown to cleave Chordin in in vitro assays (3, 23, 29) and to be capable of counteracting dorsalizing effects of Chordin in overexpression assays in *Xenopus* (23, 29) or zebrafish (3) embryos. However, genetic analysis of possible in vivo involvement of vertebrate BMP-1/Tolloid-related proteases in BMP signaling has been limited to a demonstration that the zebrafish Tolloid mutation *mini fin* yields a phenotype with some similarities to that of heterozygotes of the BMP2b mutation *swirl* and reduced expression of ventrally restricted markers, suggestive of decreased BMP signaling (8). Here we have used analysis of *Bmp1*$^{-/-}$ *Tll1*$^{-/-}$ embryo cells to provide direct genetic evidence of the in vivo involvement of vertebrate BMP-1-like proteases in cleaving Chordin. Thus, at least some members of this small family of extracellular proteinases may indeed be involved in orchestrat-

ing BMP signaling with formation of the ECM in morphogenetic events.

Total absence of detectable processing of substrates such as procollagen I and Chordin in *Bmp1*$^{-/-}$ *Tll1*$^{-/-}$ MEF media suggested the feasibility of using a proteomics approach for detecting cleavage products of novel substrates via mass-spectrometric analysis of spots present on 2D gels of wild-type MEF medium but absent from 2D gels of *Bmp1*$^{-/-}$ *Tll1*$^{-/-}$ MEF medium. In the present report, we have demonstrated the successful use of this approach in identifying the proα1 chain of type XI procollagen as a novel substrate for products of *Bmp1* and *Tll1*. Interestingly, although the proα1(XI) chain is a novel substrate, evidence here that the proα1(XI) N-terminal PARP domain is cleaved by BMP-1-like proteases, while its C-propeptide is cleaved by furin-like proprotein convertases, further validates the previous surprising findings (13, 36) of cleavage by BMP-1-like and furin-like proteases of the PARP domain and C-propeptide, respectively, of the type V collagen proα1(V) chain, which is similar in domain structure to the proα1(XI) chain. Thus, these chains of the minor fibrillar collagen types V and XI are shown to be processed differently from the chains of the major fibrillar collagen types I to III, in which C-propeptides are cleaved by BMP-1-like proteases (14, 17) and N-terminal globular domains are cleaved by proteases of the ADAMTS family (6, 7, 10).

It should be noted that the proteomics approach employed in the present report involved analysis of total proteins ethanol precipitated from relatively small volumes of MEF conditioned media. In such an approach the amount of protein that can be loaded on a gel is limited by the necessity of not overloading the most abundant proteins in conditioned medium (e.g., procollagens I and III and their cleavage products). Because of this necessity, less-abundant proteins are not detected on stained 2D gels. In contrast, it seems highly likely that fractionation of proteins by various chromatographic methodologies from larger volumes of MEF media, followed by analysis of individual fractions by 2D gel electrophoresis, will allow identification of additional substrates of the *Bmp1* and *Tll1* genes. Additional substrates may also be identified through proteomics analysis of other cell types derived from *Bmp1*$^{-/-}$ *Tll1*$^{-/-}$ embryos. Clearly, proteomics approaches such as those demonstrated and discussed here will be of use in identifying novel substrates of other proteinases for which knockout mice have been generated and issues of functional redundancy have been addressed.

ACKNOWLEDGMENTS

We thank Nick Morris (Shriners Hospital for Children, Portland, Ore.) and Larry Fisher (National Institute of Dental and Craniofacial Research) for generously providing antibodies against type XI and type I collagens, respectively. We also thank Brigid L. M. Hogan for provision of heterozygous *Bmp1*-null mice and Cian Leahy, Melvin Ayala, and Sara Tufa for excellent technical assistance.

This work was supported by funds provided by the National Institutes of Health to D.S.G. (GM63471 and AR47746), by a predoctoral fellowship from the American Heart Association awarded to W.N.P., and by National Institutes of Health Predoctoral Training Grant T32 GM07215 in Molecular Biosciences to B.M.S.

REFERENCES

1. **Amano, S., I. C. Scott, K. Takahara, M. Koch, M.-F. Champliaud, D. R. Gerecke, D. R. Keene, D. L. Hudson, T. Nishiyama, S. Lee, D. S. Greenspan, and R. E. Burgeson.** 2000. Bone morphogenetic protein 1 is an extracellular processing enzyme of the laminin 5 γ2 chain. J. Biol. Chem. **275:**22728–22735.
2. **Bateman, J. F., J. J. Pillow, T. Mascara, S. Medvedec, J. A. M. Ramshaw, and W. G. Cole.** 1987. Cell-layer-associated proteolytic cleavage of the telopeptides of type I collagen in fibroblast culture. Biochem. J. **245:**677–682.
3. **Blader, P., S. Rastegar, N. Fischer, and U. Strähle.** 1997. Cleavage of the BMP-4 antagonist Chordin by zebrafish Tolloid. Science **278:**1937–1940.
4. **Bond, J. S., and R. J. Beynon.** 1995. The astacin family of metalloendopeptidases. Protein Sci. **4:**1247–1261.
5. **Clark, T. G., S. J. Conway, I. C. Scott, P. A. Labosky, G. Winnier, J. Bundy, B. L. M. Hogan, and D. S. Greenspan.** 1999. The mammalian Tolloid-like 1 gene, *Tll1*, is necessary for normal septation and positioning of the heart. Development **126:**2631–2642.
6. **Colige, A., S.-W. Li, A. L. Sieron, B. V. Nusgens, D. J. Prockop, and C. M. Lapière.** 1997. cDNA cloning and expression of bovine procollagen I N-proteinase: a new member of the superfamily of zinc-metalloproteinases with binding sites for cells and other matrix components. Proc. Natl. Acad. Sci. USA **94:**2374–2379.
7. **Colige, A., I. Vandenberghe, M. Thiry, C. A. Lambert, J. Van Beeumen, S.-W. Li, D. J. Prockop, and C. M. Lapière.** 2002. Cloning and characterization of ADAMTS-14, a novel ADAMTS displaying high homology with ADAMTS-2 and ADAMTS-3. J. Biol. Chem. **277:**5756–5766.
8. **Connors, S. A., J. Trout, M. Ekker, and M. C. Mullins.** 1999. The role of *Tolloid/mini fin* in dorsoventral pattern formation of the zebrafish embryo. Development **126:**3119–3130.
9. **Ferguson, E. L., and K. V. Anderson.** 1991. Dorsal-ventral pattern formation in the Drosophila embryo: the role of zygotically active genes. Curr. Top. Dev. Biol. **25:**17–43.
10. **Fernandes, R. J., S. Hirohata, J. M. Engle, A. Colige, D. H. Cohn, D. R. Eyre, and S. S. Apte.** 2001. Procollagen II amino propeptide processing by ADAMTS-3. J. Biol. Chem. **276:**31502–31509.
11. **Fisher, L. W., J. T. Stubbs III, and M. F. Young.** 1995. Antisera and cDNA probes to human and certain animal model bone matrix noncollagenous proteins. Acta Orthop. Scand. Suppl. **266:**61–65.
12. **Hogan, B. L. M., R. Beddington, F. Constantini, and E. Lacy.** 1994. Manipulating the mouse embryo: a laboratory manual, 2nd ed. Cold Spring Harbor Laboratory Press, Cold Spring Harbor, N.Y.
13. **Imamura, Y., B. M. Steiglitz, and D. S. Greenspan.** 1998. Bone morphogenetic protein-1 processes the NH_2-terminal propeptide, and a furin-like proprotein convertase processes the COOH-terminal propeptide of proα1(V) collagen. J. Biol. Chem. **273:**27511–27517.
14. **Kessler, E., K. Takahara, L. Biniaminov, M. Brusel, and D. S. Greenspan.** 1996. Bone morphogenetic protein-1: the type I procollagen C-proteinase. Science **271:**360–362.
15. **Lee, S., D. E. Solow-Cordero, E. Kessler, K. Takahara, and D. S. Greenspan.** 1997. Transforming growth factor-β regulation of bone morphogenetic protein-1/procollagen C-proteinase and related proteins in fibrogenic cells and keratinocytes. J. Biol. Chem. **272:**19059–19066.
16. **Lee, S.-T., E. Kessler, and D. S. Greenspan.** 1990. Analysis of site-directed mutations in human pro-α2(I) collagen which block cleavage by the C-proteinase. J. Biol. Chem. **265:**21992–21996.
17. **Li, S.-W., A. L. Sieron, A. Gertala, Y. Hojima, W. V. Arnold, and D. J. Prockop.** 1996. The C-proteinase that processes procollagens to fibrillar collagens is identical to the protein previously identified as bone morphogenic protein-1. Proc. Natl. Acad. Sci. USA **93:**5127–5130.
18. **Marqués, G., M. Musacchio, M. J. Shimell, K. Wünnenberg-Stapleton, K. W. Cho, and M. B. O'Connor.** 1997. Production of a DPP activity gradient in the early Drosophila embryo through the opposing actions of the SOG and TLD proteins. Cell **91:**417–426.
19. **Morris, N. P., J. T. Oxford, G. B. M. Davies, B. F. Smoody, and D. R. Keene.** 2000. Developmentally regulated alternative splicing of the α1(XI) collagen chain: spatial and temporal segregation of isoforms in the cartilage of fetal rat long bones. J. Histochem. Cytochem. **48:**725–741.
20. **O'Farrell, P.** 1975. High resolution two-dimensional electrophoresis of proteins. J. Biol. Chem. **250:**4007–4021.
21. **Oxford, J. T., K. J. Doege, and N. P. Morris.** 1995. Alternative exon splicing within the amino-terminal nontriple-helical domain of the rat pro-α1(XI) collagen chain generates multiple forms of the mRNA transcript which exhibit tissue-dependent variation. J. Biol. Chem. **270:**9478–9485.
22. **Pappano, W. N., I. C. Scott, T. G. Clark, R. L. Eddy, T. B. Shows, and D. S. Greenspan.** 1998. Coding sequence and expression patterns of mouse chordin and mapping of the cognate mouse *Chrd* and human *CHRD* genes. Genomics **52:**236–239.

22a. **Perkins, D. N., D. J. Pappin, D. M. Creasy, and J. S. Cottrell.** 1999. Probability-based protein identification by searching sequence databases using mass spectrometry data. Electrophoresis **20:**3551–3567.

23. **Piccolo, S., E. Agius, B. Lu, S. Goodman, L. Dale, and E. M. De Robertis.** 1997. Cleavage of Chordin by Xolloid metalloprotease suggests a role for proteolytic processing in the regulation of Spemann organizer activity. Cell **91:**407–416.
24. **Prockop, D. J., and D. J. S. Hulmes.** 1994. Assembly of collagen fibrils de

novo from soluble precursors: polymerization and copolymerization of procollagen, pN-collagen, and mutated collagens, p. 47–90. *In* P. D. Yurchenco, D. E. Birk, and R. P. Mecham (ed.), Extracellular matrix assembly and structure. Academic Press, New York, N.Y.

25. **Prockop, D. J., and K. I. Kivirikko.** 1995. Collagens: molecular biology, diseases, and potentials for therapy. Annu. Rev. Biochem. **64:**403–434.
26. **Rattenholl, A., W. M. Pappano, M. Koch, D. R. Keene, K. E. Kadler, T. Sasaki, R. Timpl, R. E. Burgeson, D. S. Greenspan, and L. Bruckner-Tuderman.** 2002. Proteinases of the bone morphogenetic protein-1 family convert procollagen VII to mature anchoring fibril collagen. J. Biol. Chem. **277:**26372–26378.
27. **Sakai, L. Y., and D. R. Keene.** 1994. Fibrillin: monomers and microfibrils. Methods Enzymol. **245:**29–52.
28. **Schönherr, E., P. Witsch-Prehm, B. Harrach, H. Robenek, J. Rauterberg, and H. Kresse.** 1995. Interaction of biglycan with type I collagen. J. Biol. Chem. **270:**2776–2783.
29. **Scott, I. C., I. L. Blitz, W. N. Pappano, Y. Imamura, T. G. Clark, B. M. Steiglitz, C. L. Thomas, S. A. Maas, K. Takahara, K. W. Y. Cho, and D. S. Greenspan.** 1999. Mammalian BMP-1/Tolloid-related metalloproteinases, including novel family member Mammalian Tolloid-Like 2, have differential enzymatic activities and distributions of expression relevant to patterning and skeletogenesis. Dev. Biol. **213:**283–300.
30. **Scott, I. C., I. L. Blitz, W. N. Pappano, S. A. Maas, K. W. Y. Cho, and D. S. Greenspan.** 2001. Homologues of twisted gastrulation are extracellular cofactors in antagonism of BMP signalling. Nature **410:**475–478.
31. **Scott, I. C., Y. Imamura, W. N. Pappano, J. M. Troedel, A. D. Recklies, P. J. Roughley, and D. S. Greenspan.** 2000. Bone morphogenetic protein-1 processes probiglycan. J. Biol. Chem. **275:**30504–30511.
32. **Steiglitz, B. M., D. R. Keene, and D. S. Greenspan.** 2002. *PCOLCE2* encodes a functional procollagen C-proteinase enhancer (PCPE2) that is a collagen-binding protein differing in distribution of expression and post-translational modification from the previously described PCPE1. J. Biol. Chem. **277:**49820–49830.
33. **Suzuki, N., P. A. Labosky, Y. Furuta, L. Hargett, R. Dunn, A. B. Fogo, K. Takahara, D. M. P. Peters, D. S. Greenspan, and B. L. M. Hogan.** 1996. Failure of ventral body wall closure in mouse embryos lacking a procollagen C-proteinase encoded by *Bmp1*, a mammalian gene related to *Drosophila* Tolloid. Development **122:**3587–3595.
34. **Takahara, K., R. Brevard, G. G. Hoffman, N. Suzuki, and D. S. Greenspan.** 1996. Characterization of a novel gene product (mammalian Tolloid-like) with high sequence similarity to mammalian Tolloid/bone morphogenetic protein-1. Genomics **34:**157–165.
35. **Takahara, K., G. E. Lyons, and D. S. Greenspan.** 1994. Bone morphogenetic protein-1 and a mammalian Tolloid homologue (mTld) are encoded by alternatively spliced transcripts which are differentially expressed in some tissues. J. Biol. Chem. **269:**32572–32578.
36. **Unsöld, C., W. N. Pappano, Y. Imamura, B. M. Steiglitz, and D. S. Greenspan.** 2002. Biosynthetic processing of the pro-$\alpha1(V)_2$pro-$\alpha2(V)$ collagen heterotrimer by bone morphogenetic protein-1 and furin-like proprotein convertases. J. Biol. Chem. **277:**5596–5602.
37. **Uzel, M. I., I. C. Scott, H. Babakhanlou-Chase, A. H. Palamakumbura, W. N. Pappano, H.-H. Hong, D. S. Greenspan, and P. C. Trackman.** 2001. Multiple bone morphogenetic protein 1-related mammalian metalloproteinases process pro-lysyl oxidase at the correct physiological site and control lysyl oxidase activation in mouse embryo fibroblast cultures. J. Biol. Chem. **276:**22537–22543.
38. **Wozney, J. M., V. Rosen, A. J. Celeste, L. M. Mitsock, M. J. Whitters, R. W. Kriz, R. M. Hewick, and E. A. Wang.** 1988. Novel regulators of bone formation: molecular clones and activities. Science **242:**1528–1534.
39. **Xu, T., P. Bianco, L. W. Fisher, G. Longenecker, E. Smith, S. Goldstein, J. Bonadio, A. Boskey, A.-M. Heegaard, B. Sommer, K. Satomura, P. Dominguez, Z. Chengyan, A. B. Kulkarni, P. G. Robey, and M. F. Young.** 1998. Targeted disruption of the biglycan gene leads to an osteoporosis-like phenotype in mice. Nat. Genet. **20:**78–82.
40. **Zhidkova, N. I., S. K. Justice, and R. Mayne.** 1995. Alternative mRNA processing occurs in the variable region of the pro-$\alpha1(XI)$ and pro-$\alpha2(XI)$ collagen chains. J. Biol. Chem. **270:**9486–9493.